

Necessity of rice resistance to planthoppers for OsEXO70H3 regulating SAMSL excretion and lignin deposition in cell walls

Di Wu , Jianping Guo , Qian Zhang , Shaojie Shi , Wei Guan , Cong Zhou , Rongzhi Chen , Bo Du , Lili Zhu  and Guangcun He 

State Key Laboratory of Hybrid Rice, College of Life Sciences, Wuhan University, Wuhan 430072, China

Summary

Author for correspondence:
Guangcun He
Email: gche@whu.edu.cn

Received: 16 November 2021
Accepted: 25 January 2022

New Phytologist (2022) 234: 1031–1046
doi: 10.1111/nph.18012

Key words: cell wall, excretion, insect resistance, *Nilaparvata lugens*, *Oryza sativa*.

- The planthopper resistance gene *Bph6* encodes a protein that interacts with OsEXO70E1. EXO70 forms a family of paralogues in rice. We hypothesized that the EXO70-dependent trafficking pathway affects the excretion of resistance-related proteins, thus impacting plant resistance to planthoppers. Here, we further explored the function of EXO70 members in rice resistance against planthoppers.
- We used the yeast two-hybrid and co-immunoprecipitation assays to identify proteins that play roles in *Bph6*-mediated planthopper resistance. The functions of the identified proteins were characterized via gene transformation, plant resistance evaluation, insect performance, cell excretion observation and cell wall component analyses.
- We discovered that another EXO70 member, OsEXO70H3, interacted with BPH6 and functioned in cell excretion and in *Bph6*-mediated planthopper resistance. We further found that OsEXO70H3 interacted with an S-adenosylmethionine synthetase-like protein (SAMSL) and increased the delivery of SAMSL outside the cells. The functional impairment of OsEXO70H3 and SAMSL reduced the lignin content and the planthopper resistance level of rice plants.
- Our results suggest that OsEXO70H3 may recruit SAMSL and help its excretion to the apoplast where it may be involved in lignin deposition in cell walls, thus contributing to rice resistance to planthoppers.

Introduction

The brown planthopper (*Nilaparvata lugens*, BPH), a monophagous sap-sucking arthropod herbivore, is considered the most destructive pest of rice (*Oryza sativa*) throughout Asia. Understanding and utilizing BPH resistance genes is considered to be the most economical and efficient strategy for BPH management. Several BPH resistance genes have been cloned and studied (Du *et al.*, 2009; Liu *et al.*, 2015; Zhao *et al.*, 2016; Hu *et al.*, 2017). *Bph14* and *Bph9* encode a nucleotide-binding and leucine-rich repeat (NLR)-containing protein (Du *et al.*, 2009; Zhao *et al.*, 2016; Hu *et al.*, 2017). *Bph3* is a cluster of three genes encoding lectin receptor kinases (OsLecRK1–OsLecRK3) (Liu *et al.*, 2015). These genes are supposed to induce immune responses and mediate downstream signalling events, but the mechanism remains unclear. *Bph6* is a new type of resistance gene encoding a previously uncharacterized protein. Current research shows that *Bph6* in rice mediates resistance to BPH through multiple signalling pathways. *Bph6* alters the action of hormones (*cZ*-type CKs, JA and SA) and positively regulates phytoalexin production. *Bph6* also functions in the physical defence against BPH attack by reinforcing the accumulation of cellulose and hemicellulose in cell walls and maintaining the cell wall thickness. BPH6 localizes to the exocyst complex and enhanced exocytosis.

It interacts with OsEXO70E1 instead of other exocyst subunits (OsSEC3, OsSEC5, OsSEC6, OsSEC8, OsSEC10, OsSEC15 and OsEXO84). Knocking down *OsExo70E1* expression would decrease the resistance of *Bph6*-NIL plants to BPH (Guo *et al.*, 2018).

Exocytosis mediated by exocysts is an important trafficking event involved in plant cell processes (Zarsky *et al.*, 2013). Disease resistance in the plant is determined by the secretion of defence proteins and antimicrobial metabolites at infection sites (Collins *et al.*, 2003; An *et al.*, 2006; Du *et al.*, 2018). The exocyst complex is composed of eight subunits (SEC3, SEC5, SEC6, SEC8, SEC10, SEC15, EXO70 and EXO84) (Hala *et al.*, 2008; Fendrych *et al.*, 2010). In contrast to one or a few copies of other subunits, EXO70 forms a family of paralogues in plants: 13 in moss (*Physcomitrella patens*), 23 in *Arabidopsis* and 47 in rice (*O. sativa*) (Chong *et al.*, 2009; Zhang *et al.*, 2010; Cvrckova *et al.*, 2012). The multiplication of EXO70 proteins in plants may partly respond to the extensive demands for unusual cargo sorting and secretory traffic, reflecting specific biological contexts and functions (Li *et al.*, 2010; Zhang *et al.*, 2010; Martin-Urdiroz *et al.*, 2016). EXO70 family genes were found to be involved in plant organ development. For instance, OsEXO70A1 is required for normal vascular bundle differentiation and primary nutrient assimilation

(Tu *et al.*, 2015). The *SR1* gene encoding the EXO70L2 protein is critical to cell division and tracheary element development in rice (Xing *et al.*, 2021). EXO70 isoforms also function in plant immunity. For instance, OsEXO70B1 acts as an essential regulator in rice immunity by interacting with the receptor-like kinase OsCERK1, an essential component for chitin reception (Hou *et al.*, 2020). OsEXO70F3/F2 specifically forms a complex with the *Magnaporthe oryzae* effector AVR-Pii and is necessary for NLR protein Pii-dependent resistance (Fujisaki *et al.*, 2015). Although EXO70 members contribute in regulating many processes important for plant development and immunity, the influence restricting herbivore attacks is still ignored.

On facing pathogens, plant cell walls form an important line of defence. Pathogens secrete an array of enzymes to collapse the cell wall polysaccharides to penetrate and colonize host tissues. To counter these attacks, plants have evolved many compounds to inhibit these enzymes and maintain and strengthen the structural integrity of the cell wall (Juge, 2006; Lagaert *et al.*, 2009). Rice upregulates cellulose, hemicellulose and lignin synthesis to strengthen cell walls to resist BPH (Guo *et al.*, 2018; He *et al.*, 2020; Shi *et al.*, 2021). One of the main components of the cell wall is lignin, which improves its rigidity and hydrophobicity. Lignin forms a protective barrier hindering mechanical penetration by pathogenic microorganisms or degradation by microbial enzymes (Walter, 1992). Lignin concentration is closely related to disease resistance (Delgado *et al.*, 2002; Bonello *et al.*, 2003; Peltier *et al.*, 2009). Lignin biosynthesis starts with the deamination of phenylalanine and involves successive hydroxylation and methylation reactions (Wout *et al.*, 2003; Barros *et al.*, 2015). *S*-adenosylmethionine synthetase (SAMS)-catalysed *S*-adenosylmethionine (SAM) acts as a methyl donor involved in numerous transmethylation reactions including the synthesis of lignin monomers (Takusagawa *et al.*, 1996; Kota *et al.*, 2004; Roje, 2006). It has been claimed that SAMS is preferentially accumulated in lignified cells in the tomato xylem and dermal tissue (Sanchez-Aguayo *et al.*, 2004). A mutation in the *Arabidopsis* SAMS3 results in high free methionine and decreased lignin content (Shen *et al.*, 2002). These observations indicate that SAMS contributes to lignification in the secondary cell wall biosynthesis.

The finding that BPH6 associated with OsEXO70E1 paves the way for exploring the role of EXO70 in insect resistance. So, we further screened BPH6-binding proteins from EXO70 paralogues. This study identified another EXO70 member, OsEXO70H3, which interacts with BPH6 and has a positive role in *Bph6*-mediated BPH resistance. Further, we found *S*-adenosylmethionine synthase-like (SAMS_L) that interacts with OsEXO70H3 from the apoplastic proteome. OsEXO70H3 recruits SAMS_L and promotes the delivery of SAMS_L into the cell exterior. *OsExo70H3*-RNAi transgenic plants and *samsl* mutants display significantly weakened resistance to BPH attack and decrease the lignin content in plant leaf sheaths. Our results suggest that OsEXO70H3 enhances the trafficking of SAMS_L to regulate lignin deposition, thus participating in *Bph6*-mediated resistance.

Materials and Methods

Plant materials and insects

The variety Nipponbare served as a susceptible rice control. The near-isogenic line *Bph6*-NIL, which carries the resistance gene *Bph6* from Swarnalata in genetic backgrounds of Nipponbare, was used as the transgenic receptor and a resistant rice control. The transgenic line *Bph6*-RNAi, which suppresses the expression of *Bph6* in *Bph6*-NIL plants, is susceptible to the brown planthopper (*Nilaparvata lugens* Stål, BPH). The BPH insects used for feeding plants were reared on the susceptible indica variety Taichung Native1 (TN1) at Wuhan University.

BPH resistance evaluation

Rice seeds were sown in plastic cups with a diameter of 10 cm. At the three-leaf stage, 15 well-growing and consistent seedlings per cup were kept for infestation with second- to third-instar BPH nymphs at the rate of 10 insects per seedling. When all seedlings of the susceptible Nipponbare control had died, each seedling of the transgenic lines was assigned a score of 0, 1, 3, 5, 7 or 9 according to plant state, as previously described (Huang *et al.*, 2001).

Honeydew excretion and BPH weight gain measurements

A female BPH within 1 d after emergence was preweighed and confined to a preweighed Parafilm sachet. The sachet was tied to the 35-d-old leaf sheath of each plant. After 2 d of feeding, each sachet containing the excreted honeydew of the BPH was removed from the leaf sheath of the plant, and the insect was taken from the sachet. Both the insect and the sachet were reweighed. The difference between 'before' and 'after' weights of the Parafilm sachet and the BPH were recorded as honeydew excretion and BPH weight gain, respectively. At least three replicates, each with 10 insects, were used for each cultivar or line.

Development of transgenic plants and mutants

The *OsExo70H3*-RNAi construct was generated by inserting a hairpin RNAi construct from a 400-bp specific fragment of *OsExo70H3* and stuffer sequence fragment (a PDK intron) into a binary vector pCXUN (accession no. FJ905215). The construct was then transformed into *Bph6*-NIL plants using an *Agrobacterium*-mediated method to develop *OsExo70H3*-RNAi transgenic plants. The T₂ homozygous plants that contained foreign DNA integration were cultivated, and harvested for the subsequent bioassay.

The *samsl* mutants were generated using CRISPR-Cas9 technology (Ma *et al.*, 2015). The target sequence of *SAMS_L* was designed and used to generate sgRNA expression cassettes driven by the *OsU6a* promoters. The T₀ transgenic plants involving genomic targeting were confirmed by direct sequencing of PCR products. The homozygous mutant plants containing the targeted sites were selected and cultivated for bioassay.

RNA extraction and quantitative RT-PCR

The total RNAs were thoroughly isolated from leaf sheaths using TRIzol reagent (Invitrogen), as previously described (Du *et al.*, 2009). Then, 2 µg of total RNA from each sample was converted into first-strand cDNA using a PrimeScript RT Reagent Kit with gDNA Eraser (RR047Q; Takara, Kusatsu, Japan). The quantitative RT-PCR (qRT-PCR) was performed using CFX-96 Real-Time PCR system (Bio-Rad) with gene-specific primers (Supporting Information Table S1), and the iTaq Universal SYBR Green Supermix Kit (Bio-Rad).

Yeast two-hybrid assay

The Matchmaker GAL4 yeast two-hybrid system 3 (Clontech, Mountain View, CA, USA) was used to confirm protein–protein interactions. Yeast strain AH109 was cotransformed with a pair of plasmids, and serial dilutions (5×, 25× and 125×) were simultaneously plated on synthetic medium (containing an appropriate concentration of 3-amino-1,2,4-triazole (3-AT)) lacking leucine, tryptophan and histidine for colony selection, and incubated at 28°C.

Immunoblot analysis and co-immunoprecipitation

For immunoblot analysis, total proteins of rice or tobacco were extracted in extraction buffer (100 mM Tris–HCl, pH 7.5, 200 mM KCl, 20 mM MgCl₂, 2 mM EDTA, 1% Triton X-100, 5 mM DTT and 1 mM PMSF). Total proteins were separated by SDS-PAGE and detected by immunoblotting using an anti-HA antibody (M180-3; MBL, Tokyo, Japan) or an anti-Myc antibody (M192-3; MBL). For the co-immunoprecipitation (Co-IP) assays *in vivo*, rice protoplasts were extracted and transformed according to a previously described method (Zhang *et al.*, 2011). Rice protoplast cells were lysed in 300 ml extraction buffer (100 mM Tris–HCl, pH 7.5, 5 mM MgCl₂, 1 mM EDTA, 0.5% Triton X-100, 2 mM DTT and 1 mM PMSF). The soluble proteins were separated and incubated with protein G agarose (Roche) that had been bonded with 1 µg anti-Myc antibody for 3 h at 4°C. The total proteins and co-immunoprecipitated proteins were then separated by SDS-PAGE and subjected to immunoblotting using an anti-Myc antibody, an anti-HA-HRP-DirecT antibody (M180-7; MBL) or an anti-HA antibody.

Subcellular localization and bimolecular fluorescence complementation

The rice protoplast transient transformation system was utilized to express plasmids, and the pictures were captured under a laser confocal fluorescence microscope (Leica SP8, Wetzlar, Germany). For determining localization, the coding sequences of genes were amplified using gene-specific primers (Table S2) and cloned into pRHVcXFP (GFP or RFP) vectors (He *et al.*, 2018). The organelle marker bZIP63 (Walter *et al.*, 2004) represents the nucleus. The Pearson correlation coefficient (r_p) and Spearman

correlation coefficients (r_s) were obtained using the IMAGEJ program with the PSC colocalization plug-in (French *et al.*, 2008), by analysing 20 individual images for each study. In bimolecular fluorescence complementation (BiFC) assay, the DNA fragment formed by linking *Bph6* and the N-terminal of mVenus (VN) was cloned into pRHV to generate VN-BPH6. OsEXO70H3 and SAMSL were fused with the mVenus N-terminal and C-terminal of pRTVcVC and pRTVcVN, respectively (He *et al.*, 2018).

Transient expression and plasmolysis in *Nicotiana benthamiana*

For protein immunoblotting, the coding sequence of genes was cloned into pGWB17 and reconstructed pEarleyGate 100 (with HA tag). For fluorescence analysis, the coding sequence of *OsExo70H3* was cloned in the PDONR207 vector, followed by recombination into the destination vector pEarleyGate 103. The coding sequence of *SAMSL* was digested with *Xba*I and linked into the reconstructed pCAMBIA1301 vector. Each construct was introduced into the *Agrobacterium* strain GV3101 by electroporation. The transformants were incubated in MES solution (10 mM MES pH 5.7, 10 mM MgCl₂, 0.5% sucrose and 150 µM acetosyringone) for 2 h before infiltration. The *Agrobacterium* suspensions were directly injected into the 5-wk-old leaves of *Nicotiana benthamiana* (grown in a glasshouse at 25°C under a 16 h : 8 h, light : dark cycle) using a needleless syringe. After 2 d, the tobacco leaves were cut into 4-cm² pieces and treated with 6% NaCl solution for 15 min (Lam *et al.*, 2007; Wang *et al.*, 2010). The cells with fluorescent signals and plasmolysis were observed under a laser confocal fluorescence microscope (Leica SP8). The raw integrated signal density outside and inside the plasma membrane of 30 cells was measured by the IMAGEJ software. The average values of the intensity ratio were then calculated to reflect the percentages of the intensity outside the cell.

Apoplasmic protein extraction

Apoplasmic fluid was extracted according to a previous description (O'Leary *et al.*, 2014) with modifications. Thirty grams of 12-d-old rice seedlings were covered in infiltration fluids (100 mM Tris–HCl at pH 7.6, 200 mM KCl and 1 mM PMSF). A vacuum (40 kPa) for 5 min was applied three times to the seedlings. Infiltrated plants were placed in a 20-ml syringe, which was in turn inserted into a 50-ml centrifuge tube for centrifuging at 700 g (or 400 g for tobacco leaves) and 4°C for 10 min. The centrifuged fluid in the tube was recentrifuged for 5 min at 15 000 g to remove any cells or particulate matter. The apoplasmic fluid was filtered into fresh tubes through a 0.22-µm filter. The G6PDH assay kit (Solarbio, Beijing, China; BC0260) was used to test cytoplasmic contamination. The contamination rate (the ratio of enzyme activity of apoplasmic proteins to that of whole cell extracts) was < 3% (mean value of three experiments) (Alves *et al.*, 2006).

The apoplasmic fluid was concentrated using the trichloroacetic acid precipitation method. Equal amounts of apoplasmic protein were analysed by SDS-PAGE and detected by immunoblotting using an anti-Actin antibody (PPB-001; Promoter, Wuhan,

China), an anti-HA antibody (M180-3; MBL) or an anti-Myc antibody (M192-3; MBL). After measuring protein concentrations using an enhanced BCA protein assay kit (p0010S; Beyotime, Shanghai, China), the apoplastic protein was excised from gels and digested in-gel with trypsin to mass spectrometry (MS) analysis (College of Life Sciences, Wuhan University, Wuhan, China). The fold change of the mean intensities from the three replicates of *Bph6*-NIL samples over *OsExo70H3*-RNAi (RiH3-6-4) samples was calculated, and a *t*-test was applied to calculate the *P*-value. The final apoplastic proteins were defined as statistically significant if the fold change was above 2, and the *P*-value was below 0.05.

Extraction of the cell wall components

The plants at the three-leaf stage were exposed to BPH insects for 0, 1, 2 and 3 d. For polysaccharide extraction, the alcohol-insoluble residue (AIR) of the cell wall from leaf sheaths of plants was prepared as previously described (Pettolino *et al.*, 2012). The AIR was digested with α -amylase solution (α -amylase was dissolved in 10 mM Tris–maleate buffer, pH 6.9) for 12 h. Pectins were extracted with distilled water and 50 mM EDTA (pH 6.8) and boiling in water for 10 min. Hemicellulose was extracted with 24% sodium hydroxide containing 0.08% sodium borohydride at 50°C for 10 min, followed by adding acetic acid to neutralize pH and cold absolute ethanol to form a precipitate. The residual precipitate was dried and collected as the cellulose fraction. Glucose and xylose were used as calibration standards. The total sugar content of the fractions was measured at 490 nm by the phenol–sulfuric acid method (Dubois *et al.*, 1956). The crystalline cellulose content was determined at 620 nm using a modified method (Updegraff, 1969). The lignin content of leaf sheaths was measured using acetyl bromide spectrophotometry as described by Johnson *et al.* (1961).

DNA isolation and Southern blot

Rice genomic DNA was isolated with 1.5× CTAB solution (1.5% cetyl trimethyl ammonium bromide, 6.14% NaCl, 15 mM EDTA and 75 mM Tris–HCl at pH 8.0), followed by overnight digestion with restriction endonucleases *Dra*I (4 U μ g⁻¹). DNA samples on the Hybond N+ membrane (Amersham-Pharmacia, Amersham, UK) was hybridized by biotinylated hygromycin (bio-Hyg) probe and detected with a North2South Hybridization kit (17097; Thermo Scientific, Waltham, MA, USA) and a Nucleic Acid Detection Module kit (89880; Thermo Scientific).

Statistical analysis

The data were analysed by Student's *t*-test.

Oligonucleotide sequences

Primer sequences are listed in Tables S1 and S2.

Accession numbers

The sequence data from this article can be found in the GenBank and Rice Genome Annotation Project databases under the following accession numbers: *Bph6* (KX818198), *OsExo70H3* (LOC_Os12g01040), *OsExo70E1* (LOC_Os01g55799), *OsExo70A1* (LOC_Os04g58880), *OsExo70B2* (LOC_Os01g61190), *OsExo70K2* (LOC_Os07g10970), *OsExo70J1* (LOC_Os08g13570), *OsSec3A* (LOC_Os03g42750), *OsSec5* (LOC_Os04g34450), *OsSec6* (LOC_Os02g51430), *OsSec8* (LOC_Os08g22864), *OsSec10* (LOC_Os12g13590), *OsSec15A* (LOC_Os10g27990), *OsExo84B* (LOC_Os03g58970), *SAMSL* (LOC_Os07g29440), *OsPAL4* (LOC_Os02g41680), *OsPAL5* (LOC_Os04g43770), *OsPAL6* (LOC_Os04g43800), *OsPAL7* (LOC_Os05g35290), *OsCOMTL3* (LOC_Os12g13800), *OsC4H1* (LOC_Os02g26810) and *OsC4H2* (LOC_Os05g25640).

Results

OsEXO70H3 interacts with BPH6

We previously demonstrated that the rice gene *Bph6* confers a broad spectrum and robust resistance to planthoppers and encodes a novel exocyst-localized protein BPH6, which interacts with the exocyst subunit OsEXO70E1 (Guo *et al.*, 2018). The EXO70 family in rice includes 47 members (Cvrckova *et al.*, 2012). Here, we explored whether BPH6 also interacts with other OsEXO70 members. We cloned the encoding sequences of six members (*OsExo70A1*, *OsExo70B2*, *OsExo70E1*, *OsExo70H3*, *OsExo70K2* and *OsExo70J1*) from the rice variety Nipponbare and tested their interaction with BPH6 in a yeast two-hybrid assay. The yeast strain AH109 involving BPH6 and OsEXO70H3 or OsEXO70E1 grew well on SD-/Trp/-Leu/-His selective medium, but others did not (Figs 1a, S1a). The results reveal that BPH6 interacts with OsEXO70H3, as well as the previously reported OsEXO70E1. We performed yeast two-hybrid assays to examine whether OsEXO70H3 associates with other exocyst subunits. The results showed that OsEXO70H3 interacted with OsSEC3A, OsSEC5, OsSEC15A and OsEXO84B in yeast (Fig. S1b).

Though both OsEXO70H3 and OsEXO70E1 belong to the EXO70 family, they only share 20.79% of identical amino acids. *OsExo70H3* encodes for a 489 amino acid (aa) protein with an EXO70 domain between 164 and 476 aa, and *OsExo70E1* encodes for a 602 aa protein containing the EXO70 domain in the 229–593 aa region. The sequence divergence is widely distributed, but the EXO70 domain showed a higher amino acid identity (24.04%) (Fig. S1c). The considerable variation between these two EXO70 paralogues may be associated with their functional diversity (Zhang *et al.*, 2010; Cvrckova *et al.*, 2012).

To further confirm the interaction between OsEXO70H3 and BPH6, we performed a Co-IP assay in rice protoplasts. Protoplasts co-expressed OsEXO70H3-HA and BPH6-Myc constructs or expressed only the OsEXO70H3-HA construct under the control of the ubiquitin (UBI) promoter. The BPH6 protein was immunoprecipitated by an anti-Myc antibody, and OsEXO70H3-

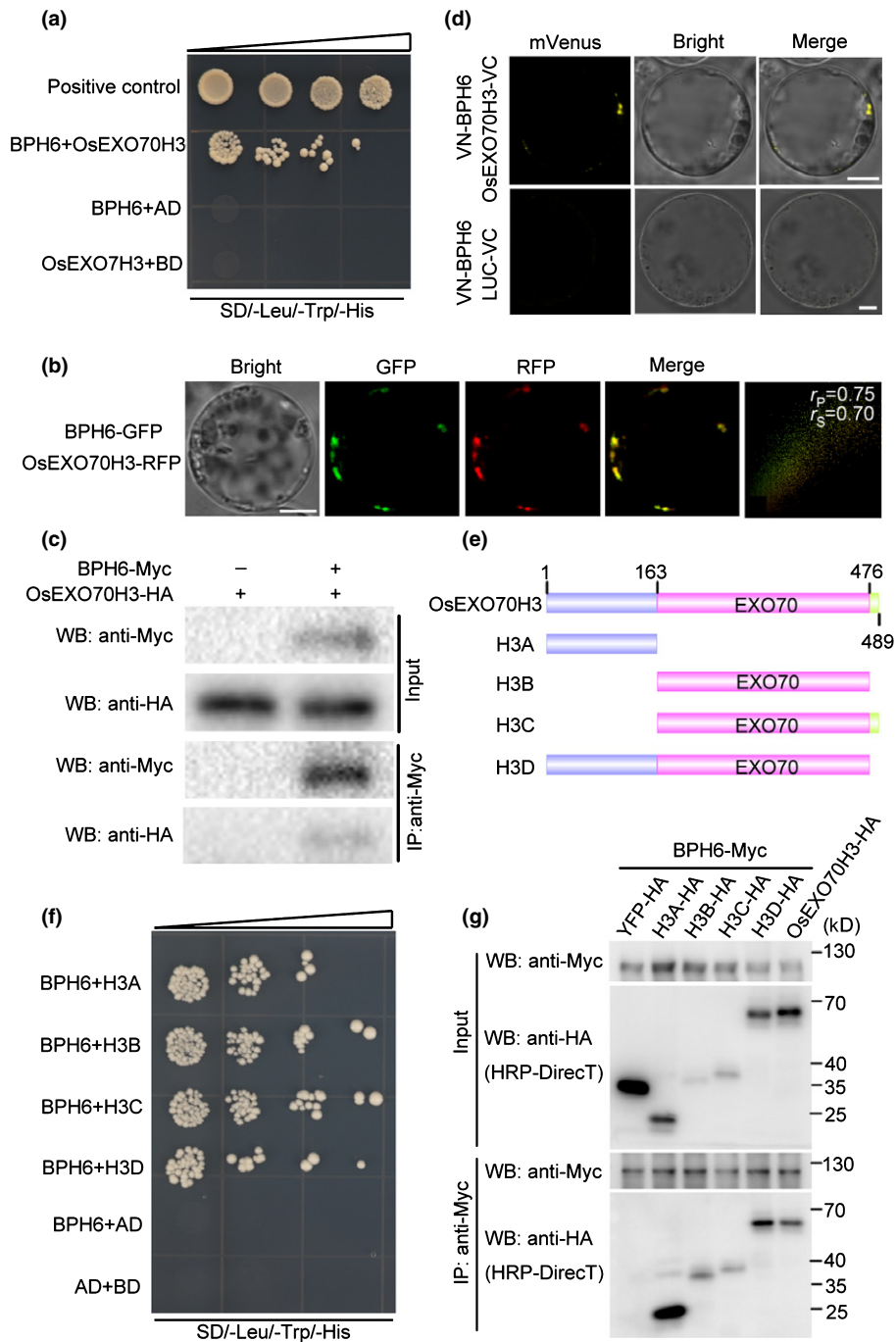


Fig. 1 BPH6 interacts with OsEXO70H3. (a) Interaction between OsEXO70H3 and BPH6 in yeast. Yeast strain AH109 cotransformed with the indicated constructs. A 5- μ l suspension (OD₆₀₀ = 0.2) of each cotransformed yeast and serial dilutions (5 \times , 25 \times and 125 \times) was dropped onto SD/-Leu/-His/-Trp selective medium. Photographs were taken after 5 d of incubation. (b) Localization of OsEXO70H3 in rice protoplasts. RFP-tagged OsEXO70H3 was cotransformed with BPH6 into protoplasts for 16–20 h. Overlapping fluorescence signals show that OsEXO70H3 colocalizes with BPH6. Values of both the Pearson correlation coefficient (r_p) and Spearman correlation coefficients (r_s) are in the range of -1 to 1 , where 0 means no correlation while $+1$ and -1 indicate strong positive and negative correlations, respectively. The values were obtained using the *IMAGEJ* software by analysing 20 individual images for each study. Bar, 5 μ m. (c) The co-immunoprecipitation (Co-IP) assay for the interaction between OsEXO70H3 and BPH6. OsEXO70H3-HA and BPH6-Myc were transiently expressed in rice protoplasts. Total protein was subjected to immunoprecipitation by an anti-Myc antibody, followed by immunoblotting with anti-HA and anti-Myc antibodies. (d) OsEXO70H3 and BPH6 interaction was examined with the bimolecular fluorescence complementation assay in rice protoplasts. Yellow fluorescence signals indicate the formation of reconstituted mVenus through the BPH6-OsEXO70H3 interaction. Control LUC-VC was used for the assay. LUC, luciferase. Bars, 5 μ m. (e) Schematic diagram of the OsEXO70H3 domain structure and the expression of fragments in the rice protoplasts (under the control of the UBI promoter). Differently coloured boxes represented individual fragments, and the relative positions of relevant amino acids are indicated. (f, g) Results of the interaction between BPH6 and the fragments of OsEXO70H3 in yeast (f) or in Co-IP (g). The anti-HA (HRP-DirecT) antibody was used to avoid the appearance of IgG. Molecular masses (in kDa) are indicated.

HA was detected only in the precipitate from rice protoplasts that co-expressed OsEXO70H3-HA and BPH6-Myc, not in the negative control that expressed OsEXO70H3-HA alone (Fig. 1c). It showed an interaction between BPH6 and OsEXO70H3. The BiFC assay was also used to test the interaction in rice protoplasts. BPH6 and OsEXO70H3 were fused with the N-terminal (VN) and C-terminal (VC) of mVenus, respectively. After cotransformation, we observed yellow fluorescent puncta in rice protoplasts (Fig. 1d), indicating that BPH6 and OsEXO70H3 interact with each other. Additionally, the OsEXO70H3-RFP signals overlapped with BPH6 in rice protoplasts (Fig. 1b), indicating that OsEXO70H3 shares the same subcellular localization with BPH6. The results confirm that OsEXO70H3 interacts with BPH6. We generated four truncated fragments of OsEXO70H3: H3A (1–163 aa), H3B (164–476 aa, the EXO70 domain), H3C (164–489 aa) and H3D (1–476 aa) (Fig. 1e) and found these fragments co-localized with BPH6 (Fig. S1d). The yeast two-hybrid assay and the Co-IP assay showed that BPH6 strongly interacted with all the truncated fragments of OsEXO70H3 *in vitro* and *in vivo* (Fig. 1f,g). The data suggest both the N-terminal and EXO70 domains bind with BPH6.

RNA interference of *OsExo70H3* decreases the *Bph6*-mediated resistance to BPH

To gain insight into the function of *OsExo70H3* in herbivore resistance, RNA interference (RNAi) technology was performed to knock down *OsExo70H3* in resistant *Bph6*-NIL plants. We selected three homozygous T₂ *OsExo70H3*-RNAi transgenic lines with single-copy insertion from 12 individual transformants for BPH resistance evaluation and further study (Fig. S2a). Quantitative RT-PCR showed that the expression of the *OsExo70H3* gene was suppressed in *OsExo70H3*-RNAi transgenic lines RiH3-6-4 and RiH3-10-3 but not in RiH3-9-7 (Fig. 2a). We examined the expression level of *OsExo70E1* in *OsExo70H3*-RNAi transgenic lines to exclude the paralogues' effects. As shown in Fig. S2b, there was no significant difference in the expression of *OsExo70E1* between *OsExo70H3*-RNAi lines and *Bph6*-NIL. This result shows that *OsExo70E1* is normally expressed in *OsExo70H3*-RNAi transgenic lines. Further, transgenic lines RiH3-6-4 and RiH3-10-3 died after infestation with BPH nymphs, while RiH3-9-7 and *Bph6*-NIL plants were still healthy, indicating that *OsExo70H3*-RNAi plants exhibited significant susceptibility to the BPH (Fig. 2b). We calculated BPH resistance scores by evaluating the state of all plants for each line. Compared with *Bph6*-NIL-resistant plants and RiH3-9-7 plants (2.82 and 3.31), the average resistance scores of RiH3-6-4 and RiH3-10-3 transgenic lines were observably higher (scores of 8.11 and 7.22, respectively) (Fig. 2c). These results indicate that knocking down *OsExo70H3* expression clearly decreases the BPH resistance of *Bph6*-NIL plants.

We further investigated the function of *OsExo70H3* in BPH resistance by measuring the weight gain and amount of honeydew secreted by the BPH insects. We found the BPH insects fed on RiH3-6-4 and RiH3-10-3 plants gained much more weight and excreted more honeydew than those fed on *Bph6*-NIL

and RiH3-9-7 plants (Figs 2d, S3a). All results show that OsEXO70H3 is required for *Bph6*-mediated BPH resistance.

Identification of SAMSL as an OsEXO70H3-binding protein

EXO70s have been reported to regulate the transport of cellular materials and be secreted along with the release of cytosolic proteins outside of the cells (Wang *et al.*, 2010; Ding *et al.*, 2014). To investigate the secretion of OsEXO70H3 *in vivo*, the OsEXO70H3-HA construct under the control of the UBI promoter was transformed into the rice variety Nipponbare. An anti-HA antibody blotting detected OsEXO70H3 in the apoplast and total proteins of transgenic plants (Fig. S4a), indicating that OsEXO70H3 was released into the plant extracellular space. To test whether BPH6 promotes the release of OsEXO70H3, OsEXO70H3-GFP was co-expressed with BPH6 or the empty vector in the leaves of *N. benthamiana*. The leaves were subjected to plasmolysis to observe OsEXO70H3 outside the cell membrane. Compared with OsEXO70H3-GFP expressed alone, we observed more OsEXO70H3-GFP fluorescent punctate dots outside the cell in the leaves of *N. benthamiana* that co-expressed OsEXO70H3 and BPH6 (Fig. 3a). We measured the ratios of the intensity of fluorescence signals outside the cell to that of total signals inside and outside of the cell to represent the amount of OsEXO70H3 secretion. As seen in Fig. 3(b), there was a significant difference in fluorescence intensity outside the cell between cells that co-expressed OsEXO70H3-GFP and BPH6 (5.45%) and those that expressed only OsEXO70H3-GFP (2.23%). Additionally, the fusion proteins were properly expressed in *N. benthamiana* (Fig. S4b). We analysed OsEXO70H3 in the apoplast of leaves co-expressing OsEXO70H3-HA and BPH6-Myc or YFP-Myc (used as control). Immunoblotting revealed that more OsEXO70H3 in apoplastic protein collected from the leaves co-expressed OsEXO70H3 with BPH6 than in control (Fig. 3c). These results indicate that BPH6 enhances the excretion of OsEXO70H3.

To seek the targets of OsEXO70H3 in *Bph6*-mediated pathways, we performed proteomics analysis using the apoplastic fluid from *OsExo70H3*-RNAi (RiH3-6-4) and *Bph6*-NIL plants exposed to BPH attack. After confirming that apoplastic extraction had negligible cytoplasmic contamination (Fig. S4c,d), MS was utilized to analyse apoplastic proteins. We identified 251 apoplastic proteins with statistically significant difference in *Bph6*-NIL samples vs RiH3 samples. Gene Ontology (GO) term analysis revealed enrichment with protein catabolism in the Molecular Function category, intracellular organelle in the Cellular Component category and oxidoreduction-related proteins in the Biological Process category (Fig. S4e). Based on the GO term analysis and Function from UniProt, Fig. S4(f) listed the representatives of three categories that may be secreted and related to resistance.

We further used the yeast two-hybrid assay to identify proteins interacting with OsEXO70H3. We found that an analogue of S-adenosylmethionine synthetase, A0A0P0X5U4 (named SAMSLike/SAMSL), interacts with OsEXO70H3 (Fig. 3d). The Co-IP and BiFC assays further confirmed the result (Fig. 3e,f). We

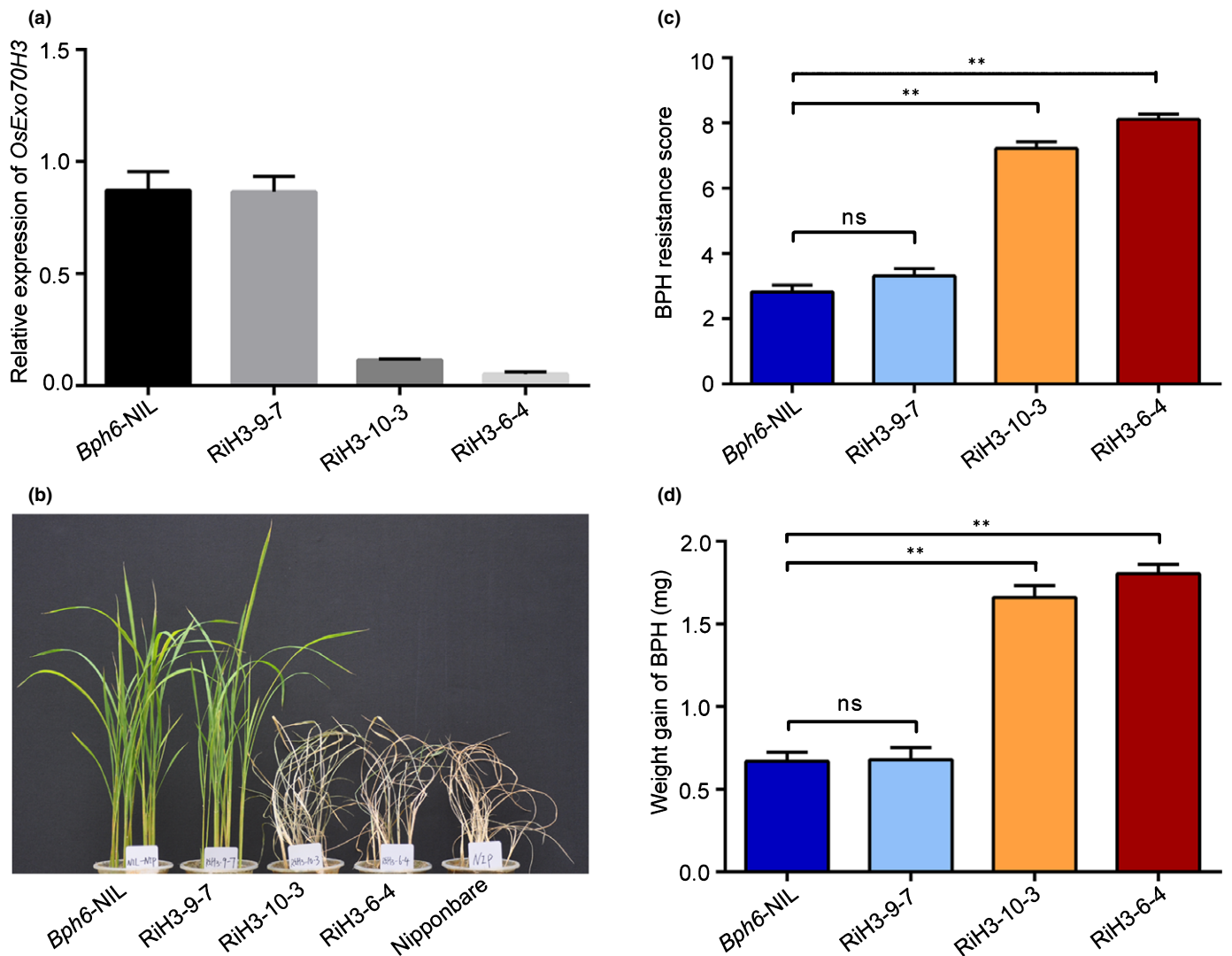


Fig. 2 BPH resistance test of *OsExo70H3*-RNAi transgenic plants. (a) The expression level of *OsExo70H3* in *Bph6*-NIL and *OsExo70H3*-RNAi T₂ transgenic lines. The cDNA used for the assay came from reverse transcription of leaf sheaths' RNA samples. Rice *UBQ* was used as a reference control. (b) BPH-resistant phenotypes of *OsExo70H3*-RNAi T₂ progenies after BPH attack. The resistant *Bph6*-NIL plants and negative control RiH3-9-7 grew well after BPH attack, while RiH3-10-3, RiH3-6-4 and Nipponbare died. (c) BPH average resistance scores of *OsExo70H3*-RNAi transgenic lines. The scores were made when all susceptible rice variety Nipponbare plants had died. Lower scores correspond to higher levels of insect resistance (three biologically independent experiments, with each replicate having 15 seedlings per rice line) ± SE. (d) Weight gain of BPH insects on *Bph6*-NIL and *OsExo70H3*-RNAi transgenic plants after 2 d. Three independent experiments with 10 BPH insects per replicate ± SE. RiH3-10-3 and RiH3-6-4, independent positive *OsExo70H3*-RNAi T₂ progenies; RiH3-9-7, negative transgenic control; Nipponbare, susceptible control; *Bph6*-NIL, the transgenic receptor for *OsExo70H3*-RNAi; BPH, the brown planthopper (*Nilaparvata lugens*). ns, not significant; **, $P < 0.01$; Student's *t*-test.

observed the localization of SAMSL in rice cells using the protoplast transient expression system. When SAMSL-GFP was expressed alone in protoplasts, it gave rise to diffuse signals throughout the cytoplasm and nucleus. However, when co-expressed with *OsEXO70H3*, SAMSL signals colocalized with *OsEXO70H3* (Fig. 3g). The result suggests that *OsEXO70H3* recruits SAMSL. To study which region of *OsEXO70H3* is associated with SAMSL, we first cotransformed SAMSL-GFP and four fragments (H3A–H3D) of *OsEXO70H3* with RFP tag, respectively, in rice protoplasts. In contrast to H3B or H3C, H3A and H3D fully colocalized with SAMSL (Fig. S5a). In addition, the yeast two-hybrid and Co-IP assays showed that SAMSL interacted with the fragments H3A (1–163 aa) and H3D (1–476

aa) but not with H3B (164–476 aa) or H3C (164–489 aa) (Fig. S5b,c), suggesting the N-terminal region, but not the EXO70 domain of *OsEXO70H3*, binds to SAMSL.

BPH6 and *OsEXO70H3* enhance the trafficking of SAMSL

Co-expression in rice protoplasts showed the colocalization of SAMSL and BPH6 (Fig. 4a). We speculated that SAMSL also interacts with BPH6. We first performed a yeast two-hybrid assay with DNA-binding domain (BD) and activation domain (AD) fused to SAMSL and BPH6, respectively. Our result indicated that SAMSL also bound to BPH6 in yeast (Fig. 4b). We then performed a Co-IP assay in rice protoplasts. We introduced

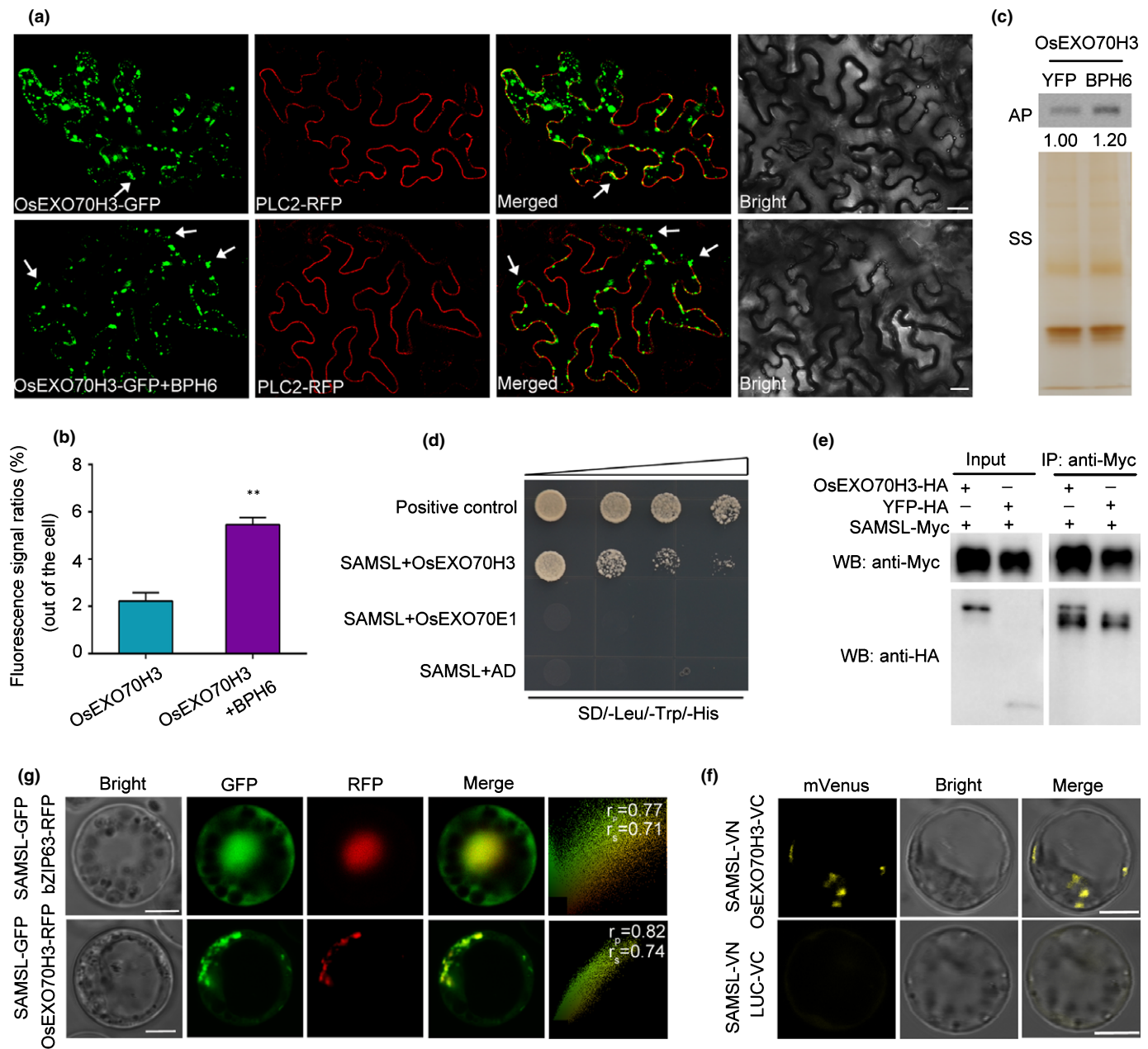


Fig. 3 Apoplastic protein SAMSLS associates with OsEXO70H3. (a) Confocal images of leaf epidermal cells of *Nicotiana benthamiana* under the state of plasmolysis. OsEXO70H3-GFP was detected outside the cell in tobacco that co-expressed the indicated pairs of vectors via the Leica Microsystems microscope. PLC2-RFP was co-expressed as a plasma membrane (PM) marker to distinguish the inside and outside of the cell. White arrows indicate green fluorescent signals outside the cell. Bars, 20 μm . (b) The percentages of OsEXO70H3-GFP fluorescence intensities outside the cell. Signal intensities of OsEXO70H3 either inside or outside the cell were quantified. (a, b) The data came from three independent experiments with 10 individual cells per replicate. Values represent means \pm SE. Asterisks indicate significant differences (**, $P < 0.01$; Student's t -test). (c) Immunoblot analysis of OsEXO70H3 in apoplastic protein (AP) of the leaves of *N. benthamiana*. OsEXO70H3-HA was co-expressed with YFP-Myc (used as control) or BPH6-Myc in tobacco leaves. OsEXO70H3 in apoplast was probed with HA antibody. The silver-stained (SS) gel shows containing proteins from the apoplast and was used to demonstrate equal loading. Band intensities determined by the IMAGEJ software were labelled below the bands. The band intensity of each sample was its ratio to the sample labelled 1.00. (d) SAMSLS selected from apoplastic proteome interacts with OsEXO70H3 in the yeast two-hybrid assay. OsEXO70H3 was fused to the activation domain (AD), and SAMSLS was fused to the DNA-binding domain (BD). The empty vector was used as a negative control. Yeast strain AH109 was introduced into different pairs of constructs. Gradient dilutions of yeast suspension were dropped onto SD/-Leu/-His/-Trp with 4 mM 3-amino-1,2,4-triazole (3-AT). (e) The Co-IP assay of SAMSLS and OsEXO70H3 from the rice protoplasts transiently co-expressing SAMSLS-Myc with OsEXO70H3-HA or YFP-HA. Immunoprecipitation with anti-Myc antibody caused OsEXO70H3-HA to coprecipitate with SAMSLS-Myc. YFP-HA was used as negative control. (f) The interaction of SAMSLS with OsEXO70H3 in the protoplast bimolecular fluorescence complementation assay. Bars, 5 μm . (g) The localization of SAMSLS in rice protoplasts. GFP-tagged SAMSLS were co-expressed with OsEXO70H3. bZIP63-RFP was used as a nucleus marker. The degree of colocalization was quantified and represented by the Pearson correlation coefficient (r_p) and Spearman correlation coefficients (r_s), where the values of +1.0 represent complete colocalization. Bars, 5 μm .

SAMSL-HA and BPH6-Myc in rice protoplasts and measured SAMSL-HA in the precipitate, with the BPH6-Myc immunoprecipitated by the anti-Myc antibody (Fig. 4c). In the BiFC assay, we detected clear yellow fluorescent signals in transfected protoplasts, indicating the formation of reconstituted mVenus through the SAMSL–BPH6 interaction (Fig. 4d). Taken together, these results prove that SAMSL and BPH6 interact with each other.

We identified the SAMSL protein through apoplastic proteomics analysis and found SAMSL interacts with OsEXO70H3 and BPH6. Therefore, we proposed that BPH6 and OsEXO70H3 function in the trafficking of SAMSL. The SAMSL-Myc construct under the control of the UBI promoter was introduced into the rice variety Nipponbare by an *Agrobacterium*-mediated transformation to test the delivery of SAMSL in plants. We next extracted the apoplastic proteins of SAMSL-Myc transgenic plants and found full-length SAMSL can be successfully transported into the apoplast (Fig. S6a). Furthermore, as previously mentioned, we constructed a SAMSL-GFP vector under the control of the 35S promoter. We then performed transient expression system in *N. benthamiana* using tobacco leaves simultaneously harbouring SAMSL-GFP and an empty vector, SAMSL-GFP and BPH6, SAMSL-GFP and OsEXO70H3, or SAMSL-GFP, BPH6 and OsEXO70H3, respectively. PLC2-RFP was co-expressed as a PM marker to distinguish the inside and outside of the cell. Tobacco cells were first subjected to an osmotic treatment with NaCl solution so that the PM would retract from the cell wall, followed by confocal imaging. The green punctate fluorescence of SAMSL-GFP was seen clearly separated from the PM. It is noteworthy that the number of SAMSL-positive signals outside the cell was markedly increased when the cells were cotransfected with SAMSL-GFP and OsEXO70H3. Similarly, there were more fluorescent punctate dots outside the cell co-expressing SAMSL-GFP and BPH6 than cells expressing SAMSL-GFP alone (Fig. 4e). In addition, the rank order of the relative fluorescence intensity of SAMSL-GFP outside of the cell was highest when it was expressed together with BPH6 and OsEXO70H3 (10%), slightly lower with OsEXO70H3 (6.97%), lower still with BPH6 (5.81%) and least when expressed alone (4.21%) (Fig. 4f). The apoplastic protein immunoblotting revealed that BPH6 and OsEXO70H3 contributed to SAMSL accumulation in the apoplast of tobacco leaves (Fig. 4g). All of the fusion proteins were properly expressed (Fig. S6b). All data indicate that SAMSL is transported into the apoplast and that OsEXO70H3 and BPH6 effectively improve its trafficking.

SAMSL plays a role in *Bph6*-mediated BPH resistance

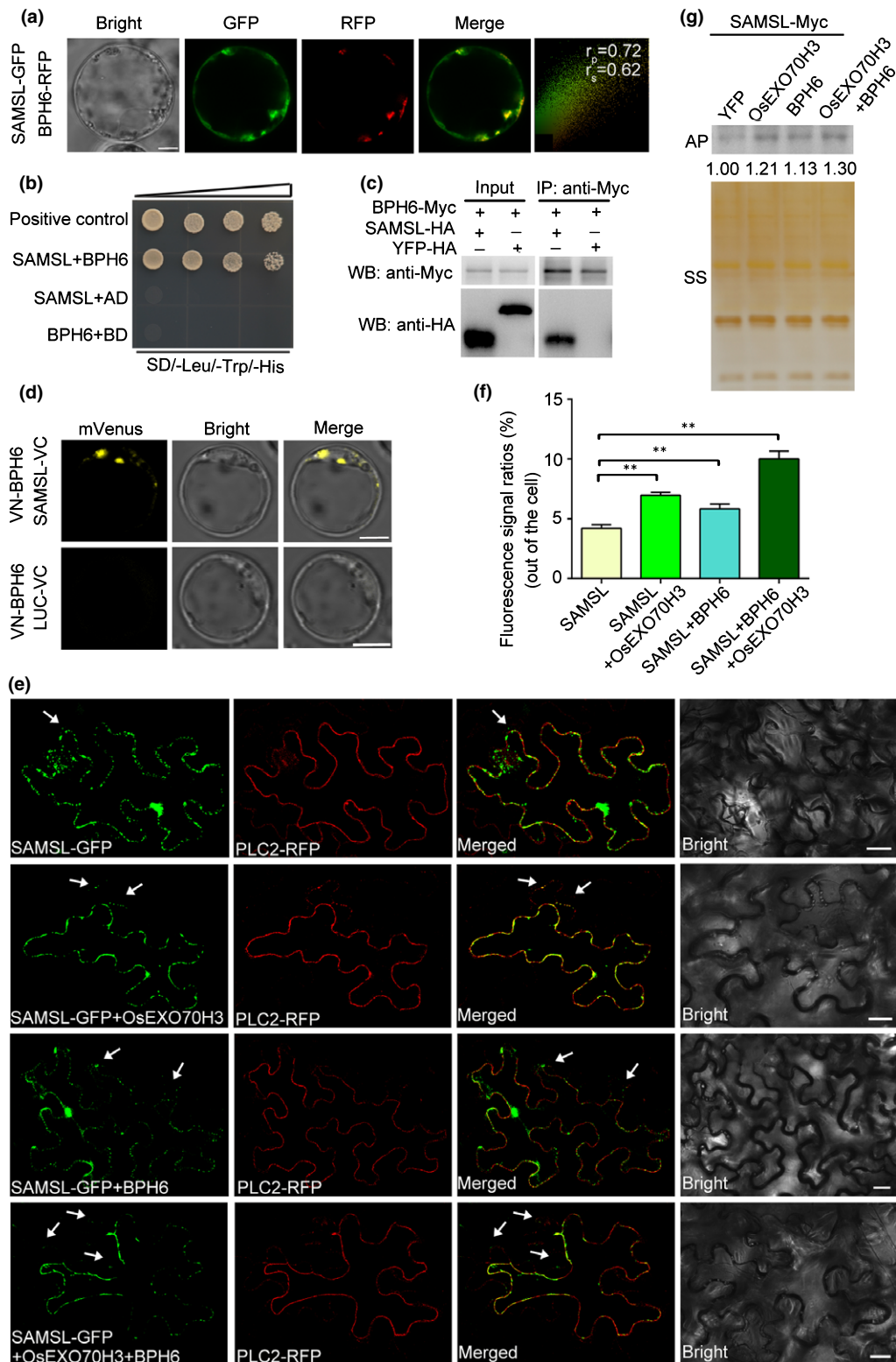
To determine whether SAMSL functions in *Bph6*-mediated insect resistance, we generated loss-of-function mutants using CRISPR/Cas9 genome editing in *Bph6*-NIL plants. We designed sgRNA specifically targeting the exon sequence, and we obtained three independent homozygous mutant plants (*samsl-5*, *samsl-10* and *samsl-19*) at the T₂ generation by DNA sequencing. DNA sequencing showed that *samsl-5* has a deletion of C at the sgRNA site, *samsl-10* has a deletion of 7 bp in the target region, and

samsl-19 has an insertion of A at the sgRNA site. By contrast, *samsl-2* has no deletion or insertion and acts as a negative control (Fig. 5a).

The *samsl* mutants were used to evaluate BPH resistance. The *samsl-5*, *samsl-10* and *samsl-19* mutants exhibited susceptibility to BPH insects, while *samsl-2* and *Bph6*-NIL plants were resistant and survived after the BPH attack (Fig. 5b). When susceptible Nipponbare plants were killed by BPH, the average resistance scores for *samsl-2* and *Bph6*-NIL were 2.91 and 2.29, respectively. Conversely, the *samsl-5*, *samsl-10* and *samsl-19* mutants had almost died, whose average resistance scores were 7.24, 7.2 and 6.07, respectively (Fig. 5c). Generally, the growth rates of insects and the quantity of honeydew secreted by BPH insects were much higher when fed on mutant lines than on resistant plants (Figs 5d, S3b). All data immediately reveal that knockout of *SAMSL* gene decreases the resistance of *Bph6*-NIL plants to BPH, and *SAMSL* plays a vital role in BPH resistance mediated by *Bph6*.

OsEXO70H3 and SAMSL function in lignin deposition

The finding that OsEXO70H3 is involved in *Bph6*-mediated resistance prompted us to check the expression levels of *OsExo70H3* in rice plants infested with BPH. The qRT-PCR analysis showed that the expression was suppressed in *Bph6*-RNAi plants but was unchanged in *Bph6*-NIL plants after BPH infestation (Fig. S7), suggesting that OsEXO70H3 activity is inhibited in susceptible plants while it remains normal in *Bph6*-expressing plants after BPH infestation. EXO70 proteins play a crucial role in numerous vital cell functions, especially in the formation of the cell wall (Van de Meene *et al.*, 2017; Meents *et al.*, 2018). We proved that OsEXO70H3 interacts with an *S*-adenosylmethionine synthetase-like protein SAMSL. Since *S*-adenosylmethionine synthetase has been reported to affect lignin deposition (Shen *et al.*, 2002; Jin *et al.*, 2017), there may be a correlation between OsEXO70H3 and lignin biosynthesis. In the lignin biosynthesis pathway, phenylalanine ammonia-lyase (PAL) is the first committed enzyme, and cinnamate 4-hydroxylase (C4H) affects PAL activity by feedback modulation (Blount *et al.*, 2000). Caffeic acid *O*-methyltransferase (COMT) is involved in the synthesis of sinapyl alcohol (Liu *et al.*, 2018). We tested the expression of these lignin-related genes in *OsExo70H3*-RNAi (RiH3-6-4) and *Bph6*-NIL plants by qRT-PCR. Concretely, the qRT-PCR analysis showed the transcript levels of the lignin biosynthesis genes (*OsPAL4*, *OsPAL5*, *OsPAL6*, *OsPAL7*, *OsCOMTL3*, *OsC4H1* and *OsC4H2*) were significantly different between resistant *Bph6*-NIL plants and *OsExo70H3*-RNAi transgenic plants (Fig. S8). We then examined the lignin content in leaf sheaths of *OsExo70H3*-RNAi transgenic line and *Bph6*-NIL plants. We found the level of lignin in *OsExo70H3*-RNAi plants to be constitutively lower than in *Bph6*-NIL plants. Generally, constant exposure to BPH insects caused a gradual decrease in lignin production in *OsExo70H3*-RNAi plants, while no such change occurred in *Bph6*-NIL plants (Fig. 6a). Additionally, we measured the cell wall polysaccharides in leaf sheaths of *OsExo70H3*-RNAi transgenic line and *Bph6*-NIL plants. The



levels of the cell wall polysaccharides were significantly lower in *OsExo70H3*-RNAi plants than in *Bph6*-NIL plants after BPH feeding (Fig. S9). The results suggest that *OsExo70H3* engages in the cell wall biosynthesis in leaf sheaths of resistant plants carrying *Bph6*.

Accordingly, our view is that SAMSL, as a target of *OsEXO70H3*, plays a role in rice resistance mediated by *Bph6*. We analysed the expression pattern of *SAMSL* in rice. We found that the level of *SAMSL* transcript was significantly induced by BPH infestation in *Bph6*-NIL plants and that this induction was

Fig. 4 The trafficking of SAMSL to the apoplast. (a) The colocalization of SAMSL and BPH6 in rice protoplasts. GFP-tagged SAMSL were co-expressed with BPH6. The Pearson correlation coefficient (r_p) and Spearman correlation coefficients (r_s) were obtained using the IMAGEJ software by analysing 20 individual images for each study. Bar, 5 μ m. (b) The yeast two-hybrid assay. SAMSL was cloned into BD vector, and BPH6 was cloned into AD vector. Yeast strain AH109 was introduced into different pairs of vectors. Gradient dilutions of yeast suspension were dropped onto SD/-Leu/-His/-Trp with 4 mM 3-amino-1,2,4-triazole (3-AT). (c) The Co-IP assay of SAMSL and BPH6 in rice protoplasts. The protoplasts transiently co-expressed BPH6-Myc with SAMSL-HA or YFP-HA. Immunoprecipitation with anti-Myc antibody caused SAMSL-HA to coprecipitate with BPH6-Myc. (d) The interaction between SAMSL and BPH6 in the bimolecular fluorescence complementation assay. Bars, 5 μ m. (e) Leaf epidermal cells of *Nicotiana benthamiana*-expressing SAMSL-GFP. SAMSL-GFP was imaged and observed by the confocal microscope outside the cell in *N. benthamiana* that co-expressed different vector combinations. The leaves of *N. benthamiana* were treated with 6% NaCl solution to maintain plasmolysis. PLC2-RFP was co-expressed as a plasma membrane (PM) marker. White arrows indicate green signals outside the cell. Bars, 20 μ m. (f) The percentages of SAMSL-GFP signal intensities outside the cell. The fluorescence signal intensity of SAMSL either inside or outside the cell was quantified in the cells. Values represent means \pm SE. (e, f) The data were derived from three independent experiments, each with 10 individual cells (**, $P < 0.01$; Student's t -test). (g) Immunoblot analysis of SAMSL in apoplastic protein (AP) of the *N. benthamiana* leaves. SAMSL in apoplast was probed with Myc antibody. The silver-stained (SS) gel shows containing proteins from the apoplast. Band intensities calculated by the ImageJ software were labelled below the bands. The sample labelled 1.00 was used as a control, and the band intensity of each sample was its ratio to the control.

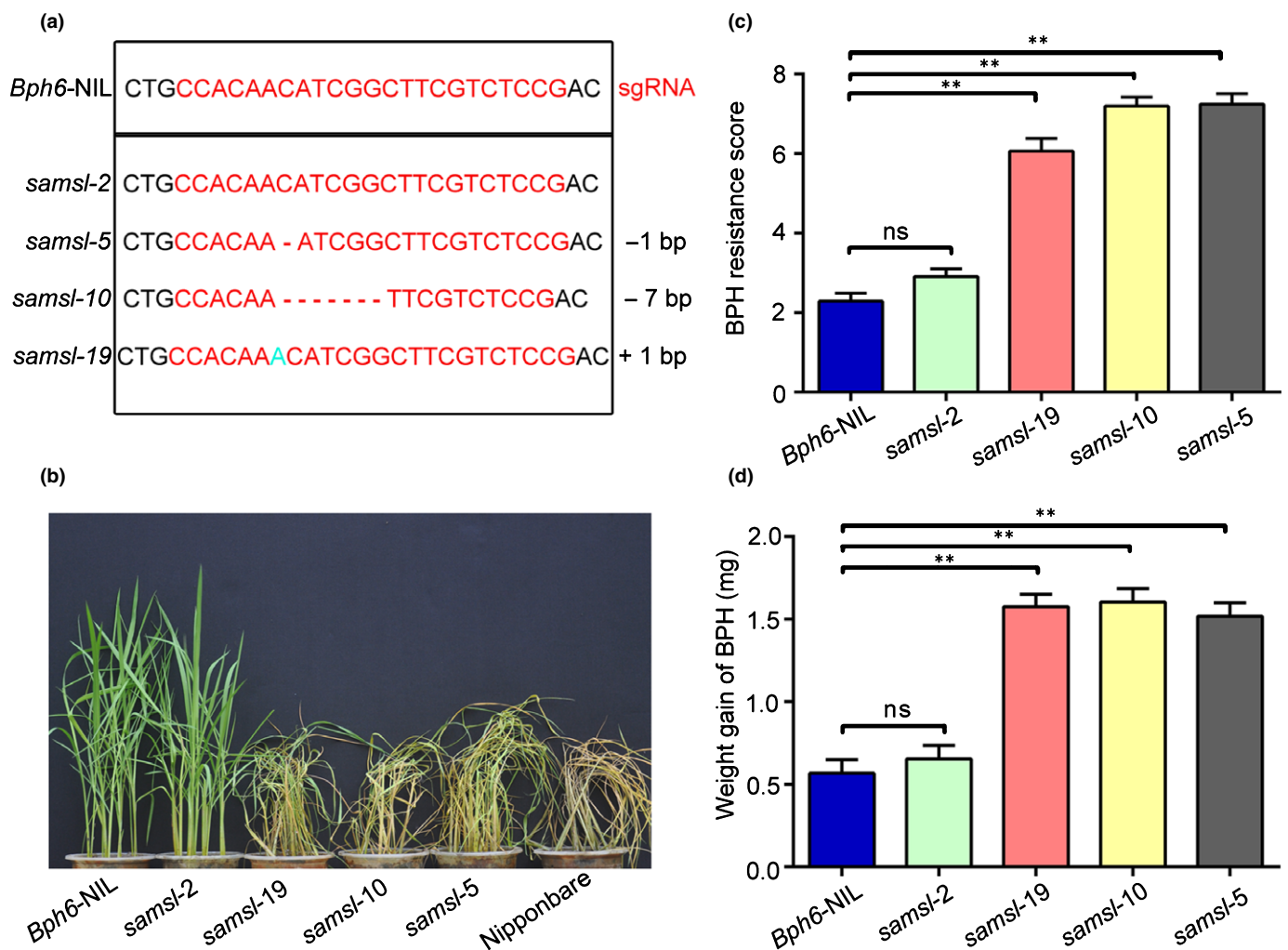


Fig. 5 BPH resistance test of *samsl* mutants. (a) DNA sequencing of *samsl* mutants. Comparison between the nucleotide sequences of SAMSL in *Bph6-NIL* and *samsl* mutants, showing that SAMSL had a deletion of C at the sgRNA site in *samsl-5* and a deletion of 7 bp in *samsl-10*. *Samsl-19* had an insertion of A in the target region. By contrast, the SAMSL in *samsl-2* shared 100% identity with *Bph6-NIL* and was used as a negative control. (b) BPH resistance phenotypes of *samsl* mutants after BPH infestation. The seedlings were exposed to BPH insects, and the photograph was taken after 7 d. The resistant *Bph6-NIL* plants and negative control *samsl-2* grew well after BPH attack, while Nipponbare and *samsl-5*, *samsl-10* and *samsl-19* died. (c) BPH average resistance scores of *samsl* mutants. Lower scores correspond to higher levels of insect resistance. The experiments were repeated three times, each time with 15 seedlings per rice line. (d) The weight gain of BPH insects on *samsl* mutants and *Bph6-NIL* plants after feeding for 2 d. Data represent means \pm SE of three independent experiments with 10 BPH insects per replicate. Asterisks indicate statistically significant differences (ns, not significant; **, $P < 0.01$; Student's t -test). *samsl-5*, *samsl-10*, *samsl-19* and independent mutant. *samsl-2*, negative transgenic control. Nipponbare, susceptible control. *Bph6-NIL*, transgenic receptor; BPH, the brown planthopper (*Nilaparvata lugens*).

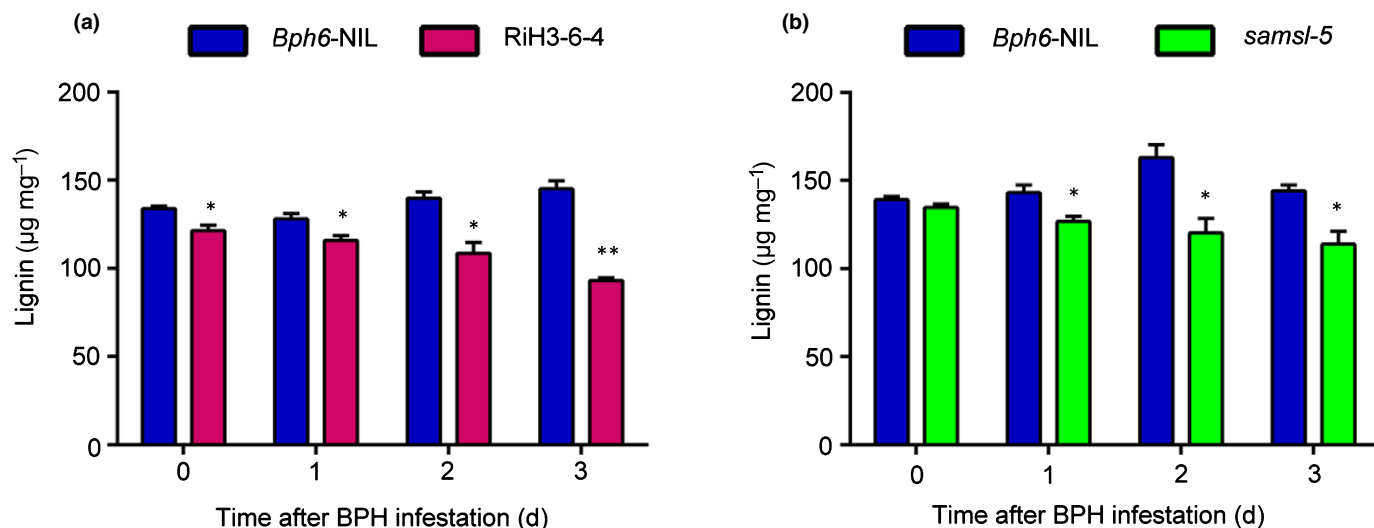


Fig. 6 Lignin content in different genotypes. (a) The lignin content in *OsExo70H3*-RNAi (*RiH3-6-4*) transgenic plants and resistant *Bph6-NIL* plants after brown planthopper (*Nilaparvata lugens*, BPH) feeding for 0, 1, 2 and 3 d. (b) The lignin content in *samsl* mutants and resistant *Bph6-NIL* plants after BPH feeding for 0, 1, 2 and 3 d. (a, b) Plants were cultured under identical conditions in plastic cups containing soil. The leaf sheaths of 15 plants for each genotype were sampled and pooled. Values are means \pm SE of three biological replicates. Asterisks indicate significant differences (*, $P < 0.05$, **, $P < 0.01$, comparison between the two groups at each time point by Student's *t*-test).

not observed in *Bph6*-RNAi plants (Fig. S7), suggesting that *Bph6* likely regulates the expression of *SAMSL* in response to BPH infestation. The lignin biosynthesis genes were also analysed in the *samsl* mutant. The qRT-PCR analysis proved that the transcript level of the genes (*OsPAL5*, *OsCOMTL3*, *OsC4H1* and *OsC4H2*) was lower in the *samsl* mutant than in *Bph6-NIL* plants (Fig. S10). After BPH attack, the lignin content was gradually reduced in the *samsl* mutant, but was unaltered in *Bph6-NIL* plants (Fig. 6b). We also found that the pectin in the *samsl* mutant was clearly less than in *Bph6-NIL* plants. Conversely, the levels of cellulose and hemicellulose were almost equal in the *samsl* mutant and *Bph6-NIL* plants and were unchanged after attack by BPH (Fig. S11). In summary, the formation and maintenance of the cell wall in *Bph6*-expressing plants exposed to BPH remain normal, but the loss of *SAMSL* function in *Bph6*-expressing plants disrupts lignin synthesis. Our data reveal that *SAMSL* is required for maintaining the synthesis and stability of lignin in *Bph6*-expressing plants.

Discussion

The EXO70 family in plants has been reported to play positive roles in plant defence against pathogens (Ostertag *et al.*, 2013; Hou *et al.*, 2020). Here, we provide evidence that *OsEXO70H3* directly regulates cell wall formation to contribute to insect resistance in rice. First, *OsEXO70H3* interacts with the resistance protein BPH6. Enhanced susceptibility of transgenic *OsExo70H3*-RNAi plants in *Bph6-NIL* background against BPH attack indicates that *OsExo70H3* positively participates in *Bph6*-mediated resistance. Next, we identified significant differences in the apoplastic proteins between *Bph6-NIL* and *OsExo70H3*-RNAi plants and discovered that the apoplastic protein *SAMSL*, an interactor of *OsEXO70H3*, was necessary for *Bph6*-mediated

resistance. Finally, the functional impairment of *OsEXO70H3* or *SAMSL* damages the transcription of lignin-related genes, resulting in the disruption of lignin deposition during BPH infestation. Hence, *OsEXO70H3* is necessary for *Bph6*-mediated resistance.

The exocyst complex is an evolutionarily conserved complex in eukaryotic organisms. However, plants possess a large number of EXO70 paralogues (Elias *et al.*, 2003; Zhang *et al.*, 2010). Various methods confirmed that plant EXO70s interact with other subunits to form a complex. The yeast two-hybrid analysis showed that *AtEXO70A1* interacts with *AtSEC3A*, *AtEXO70B1* with *AtSEC5A* and *AtEXO84B*, and *AtEXO70B2* with *AtSEC5A* and *AtSEC15B* (Hala *et al.*, 2008; Pecenkova *et al.*, 2011; Kulich *et al.*, 2013). BiFC confirmed the interactions of *AtEXO70E2* with *AtSEC6* and *AtSEC10* (Ding *et al.*, 2014). Results suggested that EXO70 paralogues function in different ways, including conventional secretion, unconventional exocytosis pathway, and the formation of novel structure EXPO, or acting independently (Fendrych *et al.*, 2010; Kulich *et al.*, 2013; Ding *et al.*, 2014; Zhang *et al.*, 2015; Hong *et al.*, 2016; Synek *et al.*, 2017; Wu *et al.*, 2017). In this study, the yeast two-hybrid assay identified that BPH6 interacts with *OsEXO70H3*. *OsEXO70H3* binds with the exocyst subunits *OsSEC3A*, *OsSEC5*, *OsSEC15A* and *OsEXO84B*. *OsEXO70H3* recruits and transports *SAMSL* into the apoplast to enhance lignin deposition, playing an important role in *Bph6*-mediated resistance. We previously identified *OsEXO70E1* functioning in BPH resistance (Guo *et al.*, 2018). BPH6 interacts with *OsEXO70E1* and enhances *OsEXO70E1*-mediated exocytosis to reinforce cell walls. Knocking down *OsExo70E1* expression in *Bph6-NIL* plants clearly decreased the resistance to BPH. Unlike *OsEXO70H3*, *OsEXO70E1* did not interact directly with *SAMSL* and did not affect the lignin content in *Bph6*-carrying

plants (Figs 3d, S12). Results suggest that these EXO70s may act on cell walls and resistance via a different pathway. The considerable divergence in amino acid sequence between these two EXO70 paralogues may be a source of their functional diversity, which needs further investigation. In *Arabidopsis*, AtRIN4 interacts with EXO70B1, EXO70E1, EXO70E2 and EXO70F1, contributing to flg22-induced callose deposition (Redditt *et al.*, 2019). It seems that EXO70 members synergistically promote plant resistance.

Any SAMS-mediated resistant response in plants is yet to be established. However, some studies suggest that SAMS may play a role in plant resistance against pathogen attacks. For example, *SbSAMS* overexpression in transgenic *Arabidopsis* plants upregulates the expression of genes responsible for pathogen and wound induction (Kim *et al.*, 2015). The expression of the *SAMS* gene was induced in parsley cells upon exposure to a fungal elicitor (Kawalleck *et al.*, 1992). Moreover, SAMSs have been reported to be involved in lignin deposition (Shen *et al.*, 2002; Jin *et al.*, 2017). Our results show that SAMS is annotated as an analogue of SAMS and *samsl* mutants display decreased lignin content. It is tempting to speculate that the SAMS protein may have the same biological function as SAMS. The knockout of the *SAMS* gene in *Bph6*-NIL weakens resistance to BPH, providing evidence supporting the putative role of SAMS in plant resistance.

That SAMSs are present in the cell wall of *Arabidopsis* is based on proteome analysis (Bayer *et al.*, 2006). The *Arabidopsis* SAMS2 protein as cytosolic cargo was recruited by the exocyst subunit EXO70E2 for transport out of the cell (Wang *et al.*, 2010). These suggest the SAMSs could be secreted to participate in cell wall formation. We identified the SAMS protein from the apoplastic proteome and found that SAMS interacts with OsEXO70H3. In the *samsl* mutant, the expression of lignin-related genes (*OsPAL5*, *OsC4H1*, *OsC4H2* and *OsCOMTL3*) encoding key enzymes in lignin biosynthesis was downregulated, which may indicate a functional linkage between SAMS and these lignin biosynthesis-related enzymes. In our apoplastic proteome, lignin biosynthesis-related enzymes such as cinnamyl alcohol dehydrogenase CAD2 and 4-coumarate-CoA ligase (4CL)-like protein were present (Fig. S4f). Therefore, we consider that SAMS could be a cofactor recruited and transported to certain enzymes to achieve lignin biosynthesis in the apoplast, establishing a barrier for the plant against insects.

Trafficking pathways deliver the cell wall-related materials to the cell membrane or into the apoplast during cell wall formation (Kim & Brandizzi, 2014; Synek *et al.*, 2014; Ebine & Ueda, 2015; Oda *et al.*, 2015; Vukasinovic *et al.*, 2017). *Arabidopsis* galactosyltransferase AtGALT31A, a cell wall-related component, colocalizes with the exocyst subunit EXO70E2, suggesting that this protein is secreted through the EXO70E2-mediated vesicle trafficking (Poulsen *et al.*, 2014). The EXO70H4-dependent secretion is responsible for callose synthase PMR4 delivery, which ensures the subsequent synthesis of the secondary cell wall. However, the *exo70H4* mutants upregulate MeJA and inhibit the growth of larvae (*Pieris brassicae* and *Spodoptera littoralis*) (Kulich *et al.*, 2015, 2018). Possibly, the influence of mutants' resistance

is hazed by other effects, probably MeJA-induced signalling pathway. In our study, BPH6 promotes the trafficking of OsEXO70H3, suggesting a direct functional link between BPH6 and OsEXO70H3-dependent trafficking. OsEXO70H3-dependent trafficking regulates the delivery of SAMS to the apoplast, resulting in lignin deposition. Interestingly, other cell wall components, including cellulose, hemicellulose and pectin, were downregulated to varying degrees when *OsExo70H3*-RNAi plants were exposed to BPH. These data suggest that OsEXO70H3 may regulate the cell wall building by recruiting other substances to vesicles. Therefore, various cell wall-related proteins may rely on OsEXO70H3-dependent trafficking to fulfil their roles in plant resistance.

The diversity of N-terminal and C-terminal motifs in EXO70s possibly mediates interactions with various cellular components to meet the demand of functional diversification. Most EXO70 proteins in the plant have a conserved C-terminal EXO70 domain (Cvrckova *et al.*, 2012). The binding of EXO70 to membrane phosphoinositides for exocyst vesicle tethering is possibly confined to C-terminal motifs (He *et al.*, 2007; Zarsky *et al.*, 2009), suggesting that the C-terminal EXO70 domain is a critical element in membrane trafficking. Since the C-terminus of OsEXO70H3 interacts with BPH6, and BPH6 increases the secretion of OsEXO70H3, we think the interaction between the C-terminal EXO70 domain and BPH6 may affect the trafficking of OsEXO70H3-mediated vesicles, thus promoting cargo transportation. Additionally, the N-terminal region of OsEXO70H3 interacts with BPH6 and SAMS. OsEXO70H3 recruits SAMS and enhances the delivery of SAMS outside the tobacco cells. Therefore, the N-terminal region is likely to play a role in the distinct function of OsEXO70H3, namely targeting unusual cargo SAMS specifically to regulate the lignin deposition in the *Bph6*-mediated signalling pathway.

We envision that, upon BPH infestation, BPH6 promotes the OsEXO70H3-dependent trafficking through protein–protein interactions. OsEXO70H3 plays a role in recruiting SAMS and enhances the trafficking of SAMS from intracellular space to the apoplast. The plant cell activates its defence machinery by depositing lignin through the continuous excretion of SAMS into the apoplast. How the downstream cell wall-associated signalling partners are activated in this process remains to be determined. Our study revealed that resistance protein deploys EXO70 to regulate the cell wall biosynthesis and promote resistance.











Acknowledgements

This work was supported by grants from the National Natural Science Foundation of China (31901518 and 31630063).

Author contributions

GH conceived and initiated the research plans. GH and DW designed the experiments. DW, JG, QZ, SS, WG, CZ, RC and BD performed the experiments. LZ prepared the experimental reagents. GH and DW analysed the data and wrote the paper.

ORCID

Rongzhi Chen  <https://orcid.org/0000-0002-0122-4415>
 Bo Du  <https://orcid.org/0000-0001-8104-3448>
 Wei Guan  <https://orcid.org/0000-0002-6503-8873>
 Jianping Guo  <https://orcid.org/0000-0001-5202-3712>
 Guangcun He  <https://orcid.org/0000-0001-6395-4774>
 Shaojie Shi  <https://orcid.org/0000-0001-7266-7152>
 Di Wu  <https://orcid.org/0000-0002-9001-139X>
 Qian Zhang  <https://orcid.org/0000-0001-6452-1153>
 Cong Zhou  <https://orcid.org/0000-0001-9841-4962>
 Lili Zhu  <https://orcid.org/0000-0001-7142-8571>

Data availability

The data that support the findings of this study are available in the Supporting Information of this article.

References

- Alves M, Francisco R, Martins I, Ricardo CPP. 2006. Analysis of *Lupinus albus* leaf apoplastic proteins in response to boron deficiency. *Plant and Soil* 279: 1–11.
- An Q, Ehlers K, Kogel KH, van Bel AJ, Huckelhoven R. 2006. Multivesicular compartments proliferate in susceptible and resistant MLA12-barley leaves in response to infection by the biotrophic powdery mildew fungus. *New Phytologist* 172: 563–576.
- Barros J, Serk H, Granlund I, Pesquet E. 2015. The cell biology of lignification in higher plants. *Annals of Botany* 115: 1053–1074.
- Bayer EM, Bottrill AR, Walshaw J, Vigouroux M, Naldrett MJ, Thomas CL, Maule AJ. 2006. *Arabidopsis* cell wall proteome defined using multidimensional protein identification technology. *Proteomics* 6: 301–311.
- Blount JW, Korth KL, Masoud SA, Rasmussen S, Lamb C, Dixon RA. 2000. Altering expression of cinnamic acid 4-hydroxylase in transgenic plants provides evidence for a feedback loop at the entry point into the phenylpropanoid pathway. *Plant Physiology* 122: 107–116.
- Bonello P, Storer AJ, Gordon TR, Wood DL, Heller W. 2003. Systemic effects of *Heterobasidion annosum* on ferulic acid glucoside and lignin of presymptomatic ponderosa pine phloem, and potential effects on bark-beetle-associated fungi. *Journal of Chemical Ecology* 29: 1167–1182.
- Chong YT, Gidda SK, Sanford C, Parkinson J, Mullen RT, Goring DR. 2009. Characterization of the *Arabidopsis thaliana* exocyst complex gene families by phylogenetic, expression profiling, and subcellular localization studies. *New Phytologist* 185: 401–419.
- Collins NC, Thordal-Christensen H, Lipka V, Bau S, Kombrink E, Qiu J-L, Hückelhoven R, Stein M, Freialdenhoven A, Somerville SC *et al.* 2003. SNARE protein-mediated disease resistance at the plant cell wall. *Nature* 425: 973–977.
- Cvrckova F, Grunt M, Bezvoda R, Hala M, Kulich I, Rawat A, Zarsky V. 2012. Evolution of the land plant exocyst complexes. *Frontiers in Plant Science* 3: 159.
- Delgado NJ, Casler MD, Grau CR, Jung HG. 2002. Reactions of smooth bromegrass clones with divergent lignin or etherified ferulic acid concentration to three fungal pathogens. *Crop Science* 42: 1824–1831.
- Ding YU, Wang J, Chun Lai JH, Ling Chan VH, Wang X, Cai YI, Tan X, Bao Y, Xia J, Robinson DG *et al.* 2014. Exo70E2 is essential for exocyst subunit recruitment and EXPO formation in both plants and animals. *Molecular Biology of the Cell* 25: 412–426.
- Du B, Zhang W, Liu B, Hu J, Wei Z, Shi Z, He R, Zhu L, Chen R, Han B *et al.* 2009. Identification and characterization of *Bph14*, a gene conferring resistance to brown planthopper in rice. *Proceedings of the National Academy of Sciences, USA* 106: 22163–22168.
- Du Y, Overdijk EJR, Berg JA, Govers F, Bouwmeester K. 2018. Solanaceous exocyst subunits are involved in immunity to diverse plant pathogens. *Journal of Experimental Botany* 69: 655–666.
- Dubois M, Gilles KA, Hamilton JK, Robers PA, Smith F. 1956. Colorimetric method for determination of sugars and related substances. *Analytical Chemistry* 28: 350–356.
- Ebine K, Ueda T. 2015. Roles of membrane trafficking in plant cell wall dynamics. *Frontiers in Plant Science* 6: 878.
- Elias M, Drdova E, Ziak D, Bavluka B, Hala M, Cvrckova F, Soukupova H, Zarsky V. 2003. The exocyst complex in plants. *Cell Biology International* 27: 199–201.
- Fendrych M, Synek L, Pecenkova T, Toupalova H, Cole R, Drdova E, Nebesarova J, Sedinova M, Hala M, Fowler JE *et al.* 2010. The *Arabidopsis* exocyst complex is involved in cytokinesis and cell plate maturation. *Plant Cell* 22: 3053–3065.
- French A, Mills S, Swarup R, Bennett M, Pridmore T. 2008. Colocalization of fluorescent markers in confocal microscope images of plant cells. *Nature Protocols* 3: 619–628.
- Fujisaki K, Abe Y, Ito A, Saitoh H, Yoshida K, Kanzaki H, Kanzaki E, Utsushi H, Yamashita T, Kamoun S *et al.* 2015. Rice Exo70 interacts with a fungal effector, AVR-Pii, and is required for AVR-Pii-triggered immunity. *The Plant Journal* 83: 875–887.
- Guo J, Xu C, Wu DI, Zhao Y, Qiu Y, Wang X, Ouyang Y, Cai B, Liu X, Jing S *et al.* 2018. *Bph6* encodes an exocyst-localized protein and confers broad resistance to planthoppers in rice. *Nature Genetics* 50: 297–306.
- Hala M, Cole R, Synek L, Drdova E, Pecenkova T, Nordheim A, Lamkemeyer T, Madlung J, Hochholdinger F, Fowler J *et al.* 2008. An exocyst complex functions in plant cell growth in *Arabidopsis* and tobacco. *Plant Cell* 20: 1330–1345.
- He B, Xi F, Zhang X, Zhang J, Guo W. 2007. Exo70 interacts with phospholipids and mediates the targeting of the exocyst to the plasma membrane. *EMBO Journal* 26: 4053–4065.
- He F, Zhang F, Sun W, Ning Y, Wang G. 2018. A versatile vector toolkit for functional analysis of rice genes. *Rice* 11: 27.
- He J, Liu Y, Yuan D, Duan M, Liu Y, Shen Z, Yang C, Qiu Z, Liu D, Wen P *et al.* 2020. An R2R3 MYB transcription factor confers brown planthopper resistance by regulating the phenylalanine ammonia-lyase pathway in rice. *Proceedings of the National Academy of Sciences, USA* 117: 271–277.
- Hong D, Jeon BW, Kim SY, Hwang J-U, Lee Y. 2016. The ROP2-RIC7 pathway negatively regulates light-induced stomatal opening by inhibiting exocyst subunit Exo70B1 in *Arabidopsis*. *New Phytologist* 209: 624–635.
- Hou H, Fang J, Liang J, Diao Z, Wang W, Yang D, Li S, Tang D. 2020. *OsExo70B1* positively regulates disease resistance to *Magnaporthe oryzae* in rice. *International Journal of Molecular Sciences* 21: 7049.
- Hu L, Wu Y, Wu DI, Rao W, Guo J, Ma Y, Wang Z, Shangguan X, Wang H, Xu C *et al.* 2017. The coiled-coil and nucleotide binding domains of BROWN PLANTHOPPER RESISTANCE14 function in signaling and resistance against planthopper in rice. *Plant Cell* 29: 3157–3185.
- Huang Z, He G, Shu L, Li X, Zhang Q. 2001. Identification and mapping of two brown planthopper resistance genes in rice. *Theoretical and Applied Genetics* 102: 929–934.
- Jin Y, Ye N, Zhu F, Li H, Wang J, Jiang L, Zhang J. 2017. Calcium-dependent protein kinase CPK28 targets the methionine adenosyltransferases for degradation by the 26S proteasome and affects ethylene biosynthesis and lignin deposition in *Arabidopsis*. *The Plant Journal* 90: 304–318.
- Johnson DB, Moore WE, Zank LC. 1961. The spectrophotometric determination of lignin in small wood samples. *TAPPI* 44: 793–798.
- Juge N. 2006. Plant protein inhibitors of cell wall degrading enzymes. *Trends in Plant Science* 11: 359–367.
- Kawalleck P, Plesch G, Hahlbrock K, Somssich IE. 1992. Induction by fungal elicitor of S-adenosyl-L-methionine synthetase and S-adenosyl-L-homocysteine hydrolase mRNAs in cultured cells and leaves of *Petroselinum crispum*. *Proceedings of the National Academy of Sciences, USA* 89: 4713–4717.
- Kim SH, Kim SH, Palaniyandi SA, Yang SH, Suh JW. 2015. Expression of potato S-adenosyl-L-methionine synthase (*SbSAMS*) gene altered

- developmental characteristics and stress responses in transgenic *Arabidopsis* plants. *Plant Physiology and Biochemistry* 87: 84–91.
- Kim SJ, Brandizzi F. 2014. The plant secretory pathway: an essential factory for building the plant cell wall. *Plant and Cell Physiology* 55: 687–693.
- Kota P, Guo D, Zubieta C, Noel J, Dixon RA. 2004. O-methylation of benzaldehyde derivatives by 'lignin specific' caffeic acid 3-O-methyltransferase. *Phytochemistry* 65: 837–846.
- Kulich I, Pecenkova T, Sekeres J, Smetana O, Fendrych M, Foissner I, Hofberger M, Zarsky V. 2013. *Arabidopsis* exocyst subcomplex containing subunit EXO70B1 is involved in autophagy-related transport to the vacuole. *Traffic* 14: 1155–1165.
- Kulich I, Vojtkova Z, Glanc M, Ortmannova J, Rasmann S, Zarsky V. 2015. Cell wall maturation of *Arabidopsis* trichomes is dependent on exocyst subunit EXO70H4 and involves callose deposition. *Plant Physiology* 168: 120–131.
- Kulich I, Vojtkova Z, Sabol P, Ortmannova J, Nedela V, Tihlarikova E, Zarsky V. 2018. Exocyst subunit EXO70H4 has a specific role in callose synthase secretion and silica accumulation. *Plant Physiology* 176: 2040–2051.
- Lagaert S, Belien T, Volckaert G. 2009. Plant cell walls: protecting the barrier from degradation by microbial enzymes. *Seminars in Cell & Developmental Biology* 20: 1064–1073.
- Lam SK, Siu CL, Hillmer S, Jang S, An G, Robinson DG, Jiang L. 2007. Rice SCAMP1 defines clathrin-coated, trans-golgi-located tubular-vesicular structures as an early endosome in tobacco BY-2 cells. *Plant Cell* 19: 296–319.
- Li S, van Os GMA, Ren S, Yu D, Ketelaar T, Emons AMC, Liu CM. 2010. Expression and functional analyses of *EXO70* genes in *Arabidopsis* implicate their roles in regulating cell type-specific exocytosis. *Plant Physiology* 154: 1819–1830.
- Liu Q, Luo L, Zheng L. 2018. Lignins: biosynthesis and biological functions in plants. *International Journal of Molecular Sciences* 19: 335.
- Liu Y, Wu H, Chen H, Liu Y, He J, Kang H, Sun Z, Pan G, Wang QI, Hu J *et al.* 2015. A gene cluster encoding lectin receptor kinases confers broad-spectrum and durable insect resistance in rice. *Nature Biotechnology* 33: 301–305.
- Ma X, Zhang Q, Zhu Q, Liu W, Chen Y, Qiu R, Wang B, Yang Z, Li H, Lin Y *et al.* 2015. A robust CRISPR/Cas9 system for convenient, high-efficiency multiplex genome editing in monocot and dicot plants. *Molecular Plant* 8: 1274–1284.
- Martin-Urdiroz M, Deeks MJ, Horton CG, Dawe HR, Jourdain I. 2016. The exocyst complex in health and disease. *Frontiers in Cell and Developmental Biology* 4: 24.
- Meents MJ, Watanabe Y, Samuels AL. 2018. The cell biology of secondary cell wall biosynthesis. *Annals of Botany* 121: 1107–1125.
- Oda Y, Iida Y, Nagashima Y, Sugiyama Y, Fukuda H. 2015. Novel coiled-coil proteins regulate exocyst association with cortical microtubules in xylem cells via the conserved oligomeric Golgi-complex 2 protein. *Plant and Cell Physiology* 56: 277–286.
- O'Leary BM, Rico A, McCraw S, Fones HN, Preston GM. 2014. The infiltration-centrifugation technique for extraction of apoplastic fluid from plant leaves using *Phaseolus vulgaris* as an example. *Journal of Visualized Experiments* 94: e52113.
- Ostertag M, Stammler J, Douchkov D, Eichmann R, Huckelhoven R. 2013. The conserved oligomeric Golgi complex is involved in penetration resistance of barley to the barley powdery mildew fungus. *Molecular Plant Pathology* 14: 230–240.
- Pecenkova T, Hala M, Kulich I, Kocourkova D, Drdova E, Fendrych M, Toupalova H, Zarsky V. 2011. The role for the exocyst complex subunits Exo70B2 and Exo70H1 in the plant–pathogen interaction. *Journal of Experimental Botany* 62: 2107–2116.
- Peltier AJ, Hatfield RD, Grau CR. 2009. Soybean stem lignin concentration relates to resistance to *Sclerotinia sclerotiorum*. *Plant Disease* 93: 149–154.
- Pettolino FA, Walsh C, Fincher GB, Bacic A. 2012. Determining the polysaccharide composition of plant cell walls. *Nature Protocols* 7: 1590–1607.
- Poulsen CP, Dilokpimol A, Mouille G, Burow M, Geshi N. 2014. Arabinogalactan glycosyltransferases target to a unique subcellular compartment that may function in unconventional secretion in plants. *Traffic* 15: 1219–1234.
- Redditt TJ, Chung E-H, Zand Karimi H, Rodibaugh N, Zhang Y, Trinidad JC, Kim JH, Zhou Q, Shen M, Dangl JL *et al.* 2019. AvrRpm1 functions as an ADP-ribosyl transferase to modify NOI domain-containing proteins, including *Arabidopsis* and Soybean RPM1-interacting protein 4. *Plant Cell* 31: 2664–2681.
- Roje S. 2006. S-adenosyl-L-methionine: beyond the universal methyl group donor. *Phytochemistry* 67: 1686–1698.
- Sanchez-Aguayo I, Rodriguez-Galan JM, Garcia R, Torreblanca J, Pardo JM. 2004. Salt stress enhances xylem development and expression of S-adenosyl-L-methionine synthase in lignifying tissues of tomato plants. *Planta* 220: 278–285.
- Shen B, Li C, Tarczynski MC. 2002. High free-methionine and decreased lignin content result from a mutation in the *Arabidopsis* S-adenosyl-L-methionine synthetase 3 gene. *The Plant Journal* 29: 371–380.
- Shi S, Wang H, Nie L, Tan D, Zhou C, Zhang Q, Li Y, Du B, Guo J, Huang J *et al.* 2021. *Bph30* confers resistance to brown planthopper by fortifying sclerenchyma in rice leaf sheaths. *Molecular Plant* 14: 1714–1732.
- Synek L, Sekeres J, Zarsky V. 2014. The exocyst at the interface between cytoskeleton and membranes in eukaryotic cells. *Frontiers in Plant Science* 4: 543.
- Synek L, Vukasinovic N, Kulich I, Hala M, Aldorfova K, Fendrych M, Zarsky V. 2017. EXO70C2 is a key regulatory factor for optimal tip growth of pollen. *Plant Physiology* 174: 223–240.
- Takusagawa F, Kamitori S, Markham GD. 1996. Structure and function of S-adenosylmethionine synthetase: crystal structures of S-adenosylmethionine synthetase with ADP, BrADP, and PPI at 28 angstroms resolution. *Biochemistry* 35: 2586–2596.
- Tu B, Hu L, Chen W, Li T, Hu B, Zheng L, Lv Z, You S, Wang Y, Ma B *et al.* 2015. Disruption of *OsEXO70A1* causes irregular vascular bundles and perturbs mineral nutrient assimilation in rice. *Scientific Reports* 5: 18609.
- Updegraff DM. 1969. Semimicro determination of cellulose in biological materials. *Analytical Biochemistry* 32: 420–424.
- Van de Meene AML, Doblin MS, Bacic A. 2017. The plant secretory pathway seen through the lens of the cell wall. *Protoplasma* 254: 75–94.
- Vukasinovic N, Oda Y, Pejchar P, Synek L, Pecenkova T, Rawat A, Sekeres J, Potocky M, Zarsky V. 2017. Microtubule-dependent targeting of the exocyst complex is necessary for xylem development in *Arabidopsis*. *New Phytologist* 213: 1052–1067.
- Walter M, Chaban C, Schütze K, Batistic O, Weckermann K, Näke C, Blazej D, Grefen C, Schumacher K, Oecking C *et al.* 2004. Visualization of protein interactions in living plant cells using bimolecular fluorescence complementation. *The Plant Journal* 40: 428–438.
- Walter MH. 1992. Regulation of lignification in defense. In: Boller T, Meins F, eds. *Genes involved in plant defense*. Vienna, Austria: Springer, 327–352.
- Wang J, Ding Y, Wang J, Hillmer S, Miao Y, Lo SW, Wang X, Robinson DG, Jiang L. 2010. EXPO, an exocyst-positive organelle distinct from multivesicular endosomes and autophagosomes, mediates cytosol to cell wall exocytosis in *Arabidopsis* and tobacco cells. *Plant Cell* 22: 4009–4030.
- Wout B, John R, Marie B. 2003. Lignin biosynthesis. *Annual Review of Plant Biology* 54: 519–546.
- Wu C, Tan L, Hooren M, Tan X, Liu F, Li Y, Zhao Y, Li B, Rui Q, Munnik T *et al.* 2017. *Arabidopsis* EXO70A1 recruits Patellin3 to the cell membrane independent of its role as an exocyst subunit. *Journal of Integrative Plant Biology* 59: 851–865.
- Xing Y, Wang N, Zhang T, Zhang Q, Du D, Chen X, Lu X, Zhang Y, Zhu M, Liu M *et al.* 2021. *SHORT-ROOT 1* is critical to cell division and tracheary element development in rice roots. *The Plant Journal* 105: 1179–1191.
- Zarsky V, Cvrckova F, Potocky M, Hala M. 2009. Exocytosis and cell polarity in plants—exocyst and recycling domains. *New Phytologist* 183: 255–272.
- Zarsky V, Kulich I, Fendrych M, Pecenkova T. 2013. Exocyst complexes multiple functions in plant cells secretory pathways. *Current Opinion in Plant Biology* 16: 726–733.
- Zhang X, Pumphlin N, Ivanov S, Harrison MJ. 2015. EXO70I is required for development of a sub-domain of the periarbuscular membrane during arbuscular mycorrhizal symbiosis. *Current Biology* 25: 2189–2195.
- Zhang Y, Liu C, Emons AM, Ketelaar T. 2010. The plant exocyst. *Journal of Integrative Plant Biology* 52: 138–146.

Zhang Y, Su J, Duan S, Ao Y, Dai J, Liu J, Wang P, Li Y, Liu B, Feng D *et al.* 2011. A highly efficient rice green tissue protoplast system for transient gene expression and studying light/chloroplast-related processes. *Plant Methods* 7: 30.

Zhao Y, Huang J, Wang Z, Jing S, Wang Y, Ouyang Y, Cai B, Xin X, Liu X, Zhang C *et al.* 2016. Allelic diversity in an NLR gene BPH9 enables rice to combat planthopper variation. *Proceedings of the National Academy of Sciences, USA* 113: 12850–12855.

Supporting Information

Additional Supporting Information may be found online in the Supporting Information section at the end of the article.

Fig. S1 Screening of the interacting proteins of BPH6.

Fig. S2 Southern blot analysis and expression level of *OsExo70H3*-RNAi transgenic plants.

Fig. S3 Honeydew excretion of BPHs insects.

Fig. S4 Sample preparation and the list of representative apoplastic proteins.

Fig. S5 The association of SAMSL and the fragments of OsEXO70H3.

Fig. S6 Immunoblotting of SAMSL in rice and tobacco leaves.

Fig. S7 Transcript analysis of *OsExo70H3* and *SAMSL* in response to BPH infestation in *Bph6*-NIL and *Bph6*-RNAi plants.

Fig. S8 Expression analysis of lignin-related genes in transgenic plants infested by BPH.

Fig. S9 The levels of cell wall polysaccharides in transgenic plants.

Fig. S10 Expression analysis of lignin-related genes in *samsl* mutants after BPH feeding.

Fig. S11 The levels of cell wall polysaccharides in *samsl* mutants.

Fig. S12 Lignin content in *OsExo70E1*-RNAi plants.

Table S1 List of quantitative RT-PCR primers used in this study.

Table S2 List of PCR primers used in this study.

Please note: Wiley-Blackwell is not responsible for the content or functionality of any Supporting Information supplied by the authors. Any queries (other than missing material) should be directed to the *New Phytologist* Central Office.